LANGMUIR

pubs.acs.org/Langmuir Article

How Detergents Dissolve Polymeric Micelles: Kinetic Pathways of Hybrid Micelle Formation in SDS and Block Copolymer Mixtures

Synne Myhre, Matthias Amann, Lutz Willner, Kenneth D. Knudsen, and Reidar Lund*

Cite This: *Langmuir* 2020, 36, 12887−12899 Read Online

ACCESS | Metrics & More | Article Recommendations | Supporting Information

ABSTRACT: Mixtures of amphiphilic polymers and surfactants are used in a wide range of applications, e.g., pharmaceuticals, detergents, cosmetics, and drug delivery systems. Still, many questions remain on how the structure and, in particular, the kinetics of block copolymer micelles are affected in the presence of surfactants and what controls the solubilization kinetics. In this work, we have studied the stability and solubilization kinetics of block copolymer micelles upon the addition of the surfactant sodium dodecyl sulfate (SDS) using small-angle X-ray/neutron scattering. The ability of the surfactant to dissolve polymer micelles or form mixed micelles has been investigated using two types of amphiphilic polymers, poly(ethylene-*alt*-propylene)−poly(ethylene oxide) (PEP1-PEO20) and *n*-alkyl-functionalized PEO (C_{28}-PEO5). The exchange kinetics of C_{28}-PEO5 micelles are in the order of hours, while PEP1-PEO20 micelles are known to be frozen on a practical timescale. In this work, we show that the addition of SDS to PEP1-PEO20 provides virtually no solubilization, even after an extended period of time. However, upon adding SDS to C_{28}-PEO5 micelles, we observe micellar dissolution and formation of mixed micelles occurring on the timescale of hours. Using a coexistence model of mixed and neat micelles, the SAXS data were analyzed to provide detailed structural parameters over time. First, we observe a fast fragmentation/fission step followed by a slow reorganization process. The latter process is essentially independent of concentration at low volume fraction but is greatly accelerated at larger concentrations. This might indicate a crossover from a predominance of molecular exchange to fusion/fission processes.

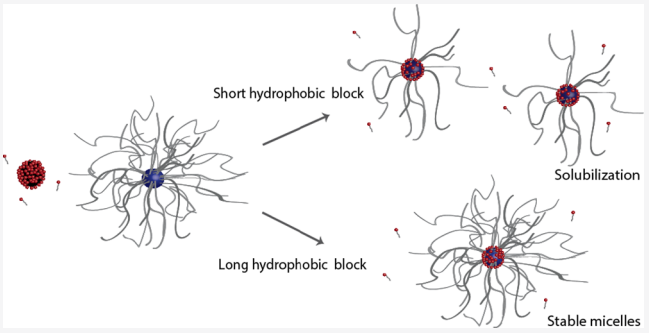

INTRODUCTION

The self-assembly of amphiphilic molecules is a highly abundant phenomenon occurring in complex structures like biological membranes as well as commercial systems, such as detergents and food products. In applications using polymer micelles, surfactants are generally present, and applications of polymer−surfactant mixtures can be found, e.g., in pharmaceutical products, detergents, paints, coatings, and cosmetic products.[1−6] With the mentioned applications and fundamental research areas in mind, an interesting question arises; when polymer micelles and surfactants mix, what are the emerging properties of the mixed system, and which properties are inherited? Previous research on polymer−surfactant interactions have been mostly dedicated to finding the final aggregation state of the mixed micelles, using static and dynamic light scattering,[1,7−9] calorimetry,[1,8,10,11] selective surfactant membrane electrodes,[11] static and dynamical NMR,[9,12] sedimentation rates,[13] fluorescence spectroscopy,[12] small-angle neutron scattering,[8] and small-angle X-ray scattering,[9] where the latter has proven to provide the most detailed structural information. A review over the field of polymer−surfactant mixtures was presented by Sastry et al.[6] It is generally reported that mixed micelles of amphiphilic block copolymers and surfactants become progressively smaller with increasing amounts of surfactants.[1,9−11,14−18] However, the results vary,[19] and in some cases, even larger micelles are formed.[9,13,14,20,21] Extensive studies on Pluronic (PEO-poly(propylene oxide)(PPO)-PEO) triblock copolymers mixed with sodium dodecyl sulfate (SDS) and hexadecyltrimethylammonium bromide (CTAB) suggest that there are three types of structures formed depending on the amount of surfactant.[1,9,10] In the low-surfactant regime, the surfactants are inserted into the core, but little structural change is observed. In the intermediate concentration regime, the polymer micelles start to break down, and both polymer micelles and single-polymer chains (unimers) surrounded by surfactants exist. In the high-surfactant regime, only unimers surrounded by surfactants are observed. Mechanistic studies have also been performed on Pluronic micelles and bile salts, which show that depending on the hydrophobicity of the core and the concentration of bile salt, the Pluronic micelles are broken.[15−17]

Received: July 19, 2020
Revised: September 22, 2020
Published: September 22, 2020

https://dx.doi.org/10.1021/acs.langmuir.0c02123
Langmuir 2020, 36, 12887−12899

It is important to note that PPO in Pluronic micelles is not as strongly segregated as pure hydrocarbons such as PEP or PEE because of a lower interfacial tension with water, resulting, e.g., in smaller aggregation numbers and faster exchange kinetics. This may also have an effect on the formation of mixed surfactant/block copolymer micelles.

It is well known that the surfactant can alter the structure of the polymer micelles. However, there is a lack of studies addressing the kinetic pathways and the structural evolution over time. Central questions are: what processes control the solubilization kinetics, and how is the exchange kinetics affected by the presence of surfactants? Surfactant micelles are known to exchange molecules, i.e., chain exchange, on a timescale of submicroseconds,[22−24] while amphiphilic block copolymers with long hydrophobic blocks have much slower chain exchange.[25−28] It is known that cosolvents, which lower the interfacial tension between the hydrophobic block and the solvent, accelerate the process of unimer exchange in micellar systems.[25,26] An interesting question is whether surfactants may show a similar effect by lowering the barrier for exchange. Understanding the solubilization kinetics may provide knowledge of the stability of polymeric micelles and answer why some micelles grow into larger micelles upon the addition of surfactant, whereas some break down into smaller mixed micelles. A study using fluorescence spectroscopy to probe the exchange kinetics of polymer−surfactant mixtures by van Stam et al.[29] found that the rate of unimer exchange is accelerated by surfactants to the same extent as with cosolvents. Schantz et al.[30] used time-resolved SANS (TR-SANS) to deduce acceleration of the polymer chain exchange in a PEE-PEO system in the presence of surfactants and suggested that this occurs through fusion/fission processes and not by unimer chain exchange that is normally the dominating mechanism.[25−28,31] Hecht et al.[32] studied the relaxation rate by light scattering in a system of Pluronic micelles and SDS or DTAB (dodecyltrimethylammonium bromide) and found that the fast relaxation constant can be ascribed to unimer exchange which increases at elevated surfactant concentrations. To the best of our knowledge, only two studies have explored the *solubilization kinetics* of amphiphilic polymeric micelles through the addition of a surfactant. Cerritelli et al.[33] used fluorescence spectroscopy and turbidity measurements to investigate di- and triblock copolymers of the type poly(ethylene oxide)−*bl*-poly(propylene sulfide) (PEO-PPS), which forms mixtures of micelles and rods, upon the addition of a nonionic surfactant, Triton X-100. These authors found first-order kinetics with respect to the surfactant concentrations. They suggest that only single surfactants and not micelles interact with the polymer structures based on the observation that the rate of break down drastically leveled off at the critical micelle concentration (cmc). They also found that the solubilization rate is faster for more hydrophobic polymers, which was explained in terms of an enhanced driving force for insertion. Cantú et al.[14] investigated the formation of mixed micelles by time-resolved light scattering measurements of mixtures of Triton X-100 and sodium cholate and two biological amphiphiles. The obtained intensity was constant with time, which was interpreted in terms of the formation of mixed micelles having already occurred before the first measurements or being extremely slow. However, since all these studies have been performed using techniques that do not provide a nanostructural resolution, it is desirable to investigate the hybridization kinetics using methods with suitable time and length resolution.

Here, we apply small-angle X-ray/neutron scattering (SAXS/SANS) to study the kinetic pathway of micellar solubilization. Small-angle scattering (SAS) techniques allow for detailed structural information between 1 and 100 nm[34] and a time resolution down to milliseconds,[35] making it a very powerful tool to investigate soft matter systems and their equilibrium and nonequilibrium kinetics. The aim of the present contribution is to quantify the controlling parameters for fast and slow solubilization and determine the mechanistic steps of the process. The model system used consists of SDS and two block copolymers with different lengths of the blocks and both make star-like micelles: the *n*-alkyl-poly(ethylene oxide) polymer, C_{28}-PEO5, and poly(ethylene-*alt*-propylene)−poly(ethylene oxide), PEP1-PEO20. Both block copolymers have been extensively studied,[25−27,36−43] showing that PEP1-PEO20 exhibits frozen molecular exchange kinetics[25,26] that can only be activated by adding dimethylformamide (DMF) as a cosolvent to lower the interfacial tension.[26] *n*-Alkyl-PEO polymers are structural hybrids between nonionic surfactants and block copolymers. In water, they form well-defined micelles with a fully segregated *n*-alkyl core. Because of the short hydrophobic block, the micelles show active chain exchange kinetics. Therefore, these micelles can be considered as "living micelles" in contrast to PEP-PEO in water. For example, the characteristic times for the exchange of C_{28}-PEO5 are in the order of 1−10 h, depending on temperature.[41] Hence, comparing the two systems, PEP-PEO and C_{28}-PEO5, will provide an insight into the role of molecular chain exchange for the formation of mixed micellar systems. Moreover, we will investigate whether surfactants affect the dynamics of block copolymer micelles in a similar way as cosolvents by lowering the surface tension. Here, we address these questions using SAXS, which allows us to monitor the structural evolution over time. Moreover, SANS techniques are employed to specifically detect possible molecular exchange induced by surfactants.

EXPERIMENTAL SECTION

Polymers and Sample Preparation. The polymers hPEP1-hPEO20, dPEP1-dPEO20, and C_{28}-PEO5 used in this study were identical with those already investigated earlier.[21,32,35,36] A two-step synthesis was applied for the preparation of the PEP-PEO polymers as described in detail in ref 32. In a first step, polyisoprene was polymerized bearing a hydroxy group in the terminal position: hPI-OH. The hPI-OH polymer was subsequently saturated with hydrogen using a $Pd/BaSO_4$ catalyst. In a second step, the resulting hPEP-OH polymer was reacted with potassium naphthalenide to produce the macroinitiator PEP-O^-K^+ which was then used for the anionic polymerization of ethylene oxide (EO). The deuterated block copolymer was similarly prepared using d-isoprene, d-EO, and deuterium for the synthesis. The two polymers were produced such that they match in molecular volumes/chain length as an important prerequisite for studying chain exchange kinetics by SANS employing the kinetic zero average contrast (KZAC) technique (see the description later). C_{28}-PEO5 was synthesized in one step by ring-opening polymerization of ethylene oxide using a mixture of 1-octacosanol/potassium 1-octacosanolate as initiator. Exact polymerization conditions can be found in ref 35. All polymers were characterized by size exclusion chromatography and for the proteated polymers in addition to ^1H NMR. A summary of the polymer characteristics is given in Table 1. SDS and D_2O were bought from Sigma-Aldrich and used as received.

Mixtures of PEP1-PEO20 and SDS were prepared by making stock solutions with Millipore water into 10 mg/mL PEP1-PEO20 according to a previously used protocol[26] and mixing with the desired SDS concentrations or D_2O for the reference sample, respectively, giving a final concentration of polymer of 5.00 mg/mL. For the data presented

https://dx.doi.org/10.1021/acs.langmuir.0c02123
Langmuir 2020, 36, 12887−12899

Table 1. Overview of the Molecular Weight of Polymer Block, M_n, Repeat Unit and Surfactant Block, M, and the X-ray Scattering Length Density of Polymers and Surfactant, ρ, Used in the Experiments

polymer/ surfactant	M_n [g/mol]	M_w/M_n	d (20 °C) [g/cm^3]	M [g/mol]	ρ (X-ray) [cm^{-2}]
h-PEO	21,900	1.04	1.20	44.04	1.11×10^{11}
h-PEP	1100	1.06	0.840	70.13	8.13×10^{10}
d-PEO	23,900	1.04	1.31	48.08	
d-PEP	1400	1.06	0.906	94.39	
C_{28}PEO5	5000	1.03	0.907	393.8[a]	8.77×10^{10}
SDS tail			0.794	169.3[a]	7.72×10^{10}
SDS head			3.37	96.06[a]	3.03×10^{11}

[a]Molecular weight of octacosyl, $C_{28}H_{57}$, SDS tail, $C_{12}H_{25}$, and head group SO_4^{3-}.

in the Results and Discussion section, the polymer was mixed with 4.66 and 2.33 mg/mL SDS, giving final concentrations of 2.33 and 1.17 mg/mL, respectively.

Stock solutions with C_{28}-PEO5 and surfactants of 20.0 and 10.0 mg/mL were made with Millipore Q water and then diluted into the desired concentrations.

The solutions for SANS experiments were made of 10.0 mg/mL proteated and deuterated micelles using the procedure reported by Lund et al.[36] To match the contrast for the fully mixed proteated and deuterated micelles, the solvent was made in a composition of 63 vol % D_2O and 37 vol % H_2O, called zero average contrast (ZAC). In addition, a solution of a blend-polymer consisting of a 50:50 combination of proteated and deuterated polymers as a reference for the fully mixed state was made. Mixed micelles were formed by mixing the polymer solutions with a constant volume fraction of 0.01 of PEP1-PEO20 in the proteated and deuterated solutions, with a 4.66 mg/mL SDS solution which was also prepared in ZAC. The solutions that consist of proteated, deuterated, and a blended PEP1-PEO20 solution, respectively, were mixed with the SDS solutions in a 1:1 ratio. The mixed micellar solutions were set to equilibrate for 5 days at room temperature before the start of the measurements. The proteated and deuterated solutions were mixed with an identical volume fraction at 50:50 and inserted into the neutron beam at 20.0 °C within the first 3 min after mixing.

Small Angle X-ray Scattering. SAXS experiments of mixtures of PEP1-PEO20 and SDS were performed at the BM29 bioSAXS beamline[44] at the European Synchrotron Radiation Facility (ESRF) in Grenoble, France. The data were obtained using an energy of 12.5 keV and a detector distance of 2.87 m, covering a Q range ($Q = 4\pi \sin(\theta/2)/\lambda$), where θ is the scattering angle and λ is the X-ray wavelength) of about 0.0047 to 0.5 Å^{-1}. The data set was calibrated to an absolute intensity scale using water as a primary standard, and 40 μL samples were run through a capillary using the flow mode of the automated sample changer.[45] SAXS data were collected in 10 successive frames of 0.5 s each to monitor the radiation damage, and the data reduction was done using the standard tools at BM29.[44]

SAXS experiments of mixtures of C_{28}-PEO5 and SDS were performed on the in-house Bruker SAXS at the Norwegian Centre for X-ray Diffraction and the Scattering and Imaging REsource Centre X-rays (RECX) lab. The data were obtained using a wavelength of 1.54 Å and a detector distance of 1.07 m, covering a Q range of about 0.009 to 0.29 Å^{-1}; 1 mL of solutions was hand-mixed and inserted into the sample cell at 20 °C in the Bruker SAXS instrument and repeatedly measured for 1 h for 3 days.

Small-Angle Neutron Scattering (SANS). SANS experiments were carried out at the JEEP-II reactor at Kjeller, Norway. The detector was a 59 cm active diameter, ^{3}He-filled RISØ type detector, mounted on rails inside the evacuated detector chamber. The sample-detector distance was varied between 1.0 and 3.4 m, and the wavelengths used were 5.1 and 10.2 Å. For the data covering the whole accessible Q range, each scattering curve was composed of three independent measurements, using different wavelength−distance combinations (5.1 Å/1.0 m, 5.1 Å/3.4 m, and 10.2 Å/3.4 m). The resulting overall Q range for the experiment was 0.006−0.3 Å^{-1}. For the study of time-dependent effects, the instrument was put in the low Q range (Q = 0.006−0.015 Å^{-1}), collecting intensity patterns at regular intervals. All the measurements were normalized to the beam monitor counts (M_i) to compensate for any possible variations in the incoming beam flux. The scattering intensity profiles $d\Sigma/d\Omega(Q)$ were obtained by azimuthally averaging the processed 2D images, which were normalized using direct beam measurements with a calibrated attenuator.

THEORETICAL SECTION

Scattering Model for Coexisting Mixed and Free Micelles. The SAXS data of the mixed micelle systems were fitted on an absolute scale using a new structural model consisting of contributions from mixed micelles (MM), surfactant micelles (SM), and free surfactant chains (Sfree). The total intensity, $\frac{d\Sigma}{d\Omega}_{total}(Q)$, is given by:

$$\frac{d\Sigma}{d\Omega}_{total}(Q) = \frac{\phi_{Pol} + \phi_{SDSm}}{V_{MM}} P_{MM}(Q) + \frac{\phi_{SDSs}}{V_{SM}} P_{SM}(Q) + \frac{\phi_{SDSfree}}{V_{sfree}} P_{Sfree}(Q) \quad (1)$$

where ϕ_{Pol} is the polymer volume fraction, and $\phi_{SDSn} = \phi_{SDSm} + \phi_{SDSs} + \phi_{SDSfree}$ is the total volume fraction of the surfactant. V_{MM}, V_{SM}, and V_{Sfree} are the volumes of the mixed micelles, the surfactant micelles, and the free chains, respectively. $P_{SM}(Q)$, $P_{Sfree}(Q)$, and $P_{MM}(Q)$ are the form factor of surfactant micelles, free surfactant chains, and mixed micelles, respectively. The form factor for the mixed micelles is based on the form factor for spherical core−shell micelles.[39] In line with what is found for pure block copolymer micelles,[27,36,39] the mixed micelles are envisioned with a water-free core consisting of the hydrophobic block (C_{28} or PEP1) and the surfactant tail. On the outside, we have two regions: a shell consisting of the SDS headgroups and a corona consisting of the PEO chains. To quantify the amount of SDS in the mixed micelles, $f_{SDSm} = \phi_{SDSm}/\phi_{SDSn}$, the fraction of SDS in mixed micelles relative to the total SDS volume fraction is introduced. The aggregation number of the polymer is then calculated by:

$$N_{agg}^{P} = N_{agg} \cdot (1 - f_{SDSm} \cdot \phi_{SDSn}) \quad (2)$$

Accordingly, the aggregation number of the surfactant is calculated by:

$$N_{agg}^{s} = N_{agg} \cdot f_{SDSm} \cdot \phi_{SDS} \quad (3)$$

where N_{agg} is the total aggregation number of the micelles. Based on this model, the volume and therefore the radius of the core can be calculated by simple geometric considerations:

$$V_c = V_{c,Pol} \cdot (1 - f_{SDSm} \cdot \phi_{SDSn}) + V_{c,SDS}(f_{SDSm} \cdot \phi_{SDSn}) \quad (4)$$

$$R_c = \left(\frac{3V_c \cdot N_{agg}}{4\pi}\right)^{1/3} \quad (5)$$

where $V_{c,Pol}$ is the dry volume of the hydrophobic block of the polymer, and $V_{c,SDS}$ is the dry volume of the surfactant tail. The scattering from the mixed micelles can then be divided up into the scattering amplitudes, $A_i(Q)$, for the core, the SDS headgroups, and the PEO corona. Three terms arising from the interference between the core−corona, the core−shell, and the shell−corona weighted by the dry volume and the contrast

https://dx.doi.org/10.1021/acs.langmuir.0c02123
Langmuir 2020, 36, 12887−12899

are added to the intensity from the mixed micelle. The form factor for mixed micelles is then given by:

$$\begin{aligned} P_{MM}(Q) = {} & N_{agg}{}^2 V_c{}^2 \Delta\rho_c^2 A_c(Q)^2 + (N_{agg}^s)^2 V_{sh}{}^2 \Delta\rho_{sh}^2 A_{sh}(Q)^2 \\ & + N_{agg}^p (N_{agg}^p - B(0)) V_{PEO}{}^2 \Delta\rho_{PEO}^2 A_{PEO}(Q)^2 \\ & + 2N_{agg} N_{agg}^s V_c V_{sh} \Delta\rho_c \Delta\rho_{sh} A_c(Q) A_{sh}(Q) \\ & + 2N_{agg} N_{agg}^p V_c V_{PEO} \Delta\rho_c \Delta\rho_{PEO} A_c(Q) A_{PEO}(Q) \\ & + 2N_{agg}^p N_{agg}^s V_{sh} V_{PEO} \Delta\rho_{sh} \Delta\rho_{PEO} A_{sh}(Q) A_{PEO}(Q) \\ & + N_{agg} V_{PEO}{}^2 \Delta\rho_{PEO}^2 B(Q) \end{aligned} \quad (6)$$

where V_i is the dry volume and i: the core (c), the shell (sh), and the PEO corona (PEO). $\Delta\rho$ is the contrast between i and the solvent, $B(Q)$ is the blob scattering from the corona,[39] and $B(0) = \frac{1}{1+\nu}$, where ν is a parameter for the interaction between the PEO chains in the corona. The amplitudes, A_i, of the core and the PEO corona are given by eq 7, which are the same as for the spherical core−shell model:[39]

$$A_i(Q) = \begin{cases} \dfrac{3\sin(Q\cdot R_c) - (QR_c\cos(Q\cdot R_c))}{(QR_c)^3} \cdot \exp\left(-\dfrac{\sigma_{int}^2 Q^2}{2}\right) & \text{core} \\ \dfrac{1}{C}\displaystyle\int_{R_c}^{\infty} \mathrm{d}r \, \dfrac{4\pi r^2 r^{-4/3}}{1 + \exp\left(\frac{r - R_m}{\sigma_m R_m}\right)} \cdot \dfrac{\sin(Qr)}{Qr} \cdot \exp\left(-\dfrac{\sigma_{int}^2 Q^2}{2}\right) & \text{PEO shell} \end{cases} \quad (7)$$

where r is the radius from the center of the micelle, R_c is the core radius, R_m is the micelle radius, σ is a cutoff parameter due to the final size of the PEO chains, σ_{int} is the core−corona smearing, and C is a normalization constant which is given by eq 8.:

$$C = \int_{R_c}^{\infty} \frac{4\pi r^2 r^{-4/3}}{1 + \exp\left(\frac{r - R_m}{\sigma_m R_m}\right)} \mathrm{d}r \quad (8)$$

The SDS headgroup shell is modeled as a hollow sphere according to eq 9.

$$A_{sh}(Q) = \frac{V_{Sh\text{-}outer}\cdot A(Q, R + dR_{MM})\cdot\exp\left(-\frac{\sigma_{into}^2 Q^2}{2}\right)}{V_{sh}} - \frac{V_c\cdot A_c(Q, R_c)\cdot\exp\left(-\frac{\sigma_{int}^2 Q^2}{2}\right)}{V_{sh}} \quad (9)$$

where dR_{MM} is the thickness of the SDS headgroup shell. The amplitude from spheres with radius R is given by eq 10:

$$A_s(Q, R) = \frac{(3\sin(Q\cdot R)) - (Q\cdot R\cos(Q\cdot R))}{(Q\cdot R)^3} \quad (10)$$

Accordingly, the amplitude from the inner edge of the shell is given by inserting for R_c. The radius to the outer edge is given by $R_c + dR_{MM}$, where dR_{MM} is the thickness of the SDS headgroup shell. $V_{Sh} = 4\pi/3[(R + dR_{MM})^3 - R^3]$ is the volume of the outer shell. To account for the interfacial smearing of the SDS headgroup shell, a smearing parameter for the shell, σ_{into}, was introduced. The complete model then yields fit parameters for aggregation number N_{agg}, radius of the micelle R_m, radius of gyration R_g of the polymer chains in the corona, smearing of the core−corona interface σ_{int} and outer SDS shell/corona interface σ_{into}, shell thickness dR_{MM}, interaction parameter between the chains in the corona ν, and cutoff parameter of the corona σ. For pure SDS micelles or the mixed micelles at later and equilibrated stages, structure factor effects were present. This was accounted for by multiplying the well-known expression for the Hayter Penfold structure factor for screened electrostatic interaction to the respective terms in eq 1. Finally, the finite spread in the nominal Q of the instrument was accounted for by integrating eq 1 over the resolution function. Trial results showed that including polydispersity in the aggregation number, which is almost certainly present in the system, did not notably improve the fit quality but rather caused more ambiguity and over-parametrization. Consequently, this dispersity in size and composition was ignored for simplicity and conciseness and the fit parameters obtained must be regarded as average values.

RESULTS AND DISCUSSION

PEP1-PEO20 and SDS Mixtures. Figure 1a shows the obtained SAXS scattering data at 20 °C from the 5.0 mg/mL PEP1-PEO20 reservoir and a mixture of 5.00 mg/mL PEP1-PEO20 and 1.16 mg/mL SDS in water. The molar ratio of SDS/PEP1-PEO20, in this case, is 9.3. At low and intermediate Q, we see only minor differences in intensity between the mixed micelle and the pure PEP1-PEO20 polymer. Figure 1b shows the scattering profile after 3 min, 1 h, and 5 days, respectively,

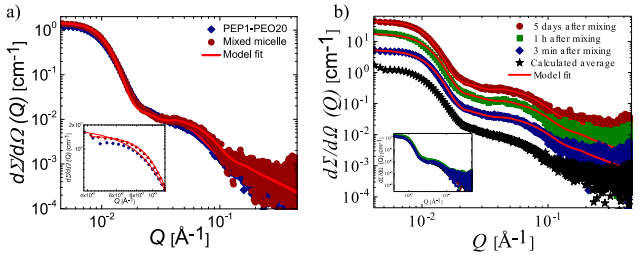

Figure 1. (a) SAXS scattering curves of 5.00 mg/mL PEP1-PEO20 with core−shell model fit, and equilibrated mixture of 5.00 mg/mL PEP1-PEO20 + 1.16 mg/mL SDS, fitted with the MM model. The inset shows the fit in the low Q region. (b) SAXS scattering curves of equilibrated 5.00 mg/mL PEP1-PEO20 mixed with 1.16 mg/mL SDS measured after 3 min, 1 h, and 5 days after mixing, compared with the calculated average. The scaling factor is (from calculated average and up) 1, 3, 15, and 30. The inset in panel (b) shows the scattering curves on an absolute scale.

https://dx.doi.org/10.1021/acs.langmuir.0c02123
Langmuir 2020, 36, 12887−12899

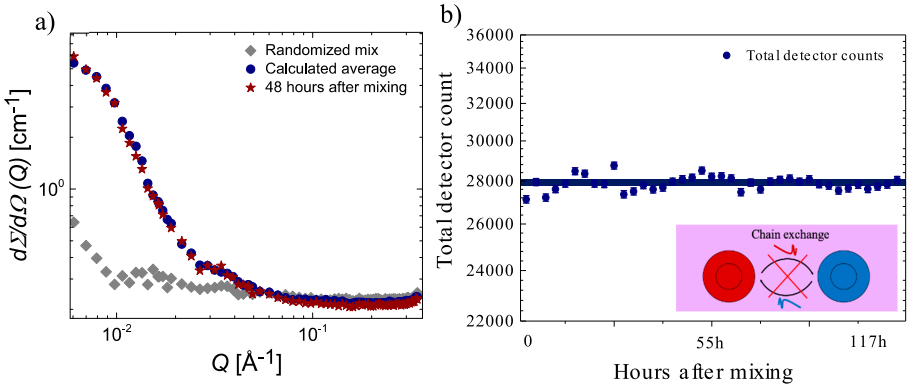

Figure 2. (a) Scattering curve from SANS of 5.00 mg/mL h-PEP1-h-PEO20 and 2.33 mg/mL SDS mixed with 5.00 mg/mL d-PEP1-d-PEO20 and 2.33 mg/mL SDS after 48 h. The figure also shows the calculated average as well as a randomized mix of the two samples. (b) Total detector count over 5 days of the same mixture as displayed in (a).

after mixing, compared with the calculated average. The reference average scattering is obtained by measuring the reservoirs at the same concentration separately and adding the intensities, which gives the theoretical scattering if there were no interactions or structural change. However, a small increase in the intensity with respect to the calculated average is seen to be present in the low Q region of the scattering data obtained 3 min after mixing (cf. inset in Figure 1b. The intensity in the low Q region in the scattering profile after 1 h and 5 days is also slightly larger than the calculated average, which indicates that the mixed micelles are larger than the initial PEP1-PEO20 micelles. In addition, a small change of the scattering curve observed in the intermediate Q region suggests a change in the core−corona interface. This indicates an increase in the aggregation number, either by a redistribution of polymer chains or insertion of SDS into the polymer micelles. The data could be consistently fitted by the mixed micelle model described in Determining the Molecular Exchange Kinetics using TR-SANS and indicated that that SDS is inserted into the PEP1-PEO20 micelles. However, it is not clear whether PEP-PEO chains are redistributed and the micelles are reorganized. Before coming back to the detailed structure of the micelles, we present results from the exchange kinetics of the mixed micelles.

To determine whether molecular exchange kinetics is active in the presence of surfactants for the PEP1-PEO20 system, we employed the kinetic zero average contrast (KZAC) SANS technique.[25,46] The method is based on mixing proteated (H) and deuterated (D) micelles in an H_2O/D_2O mixture that matches the average of the scattering length density of the two micelles and measuring the time-dependent neutron intensity. At time t = 0, the contrast and, consequently, the scattered intensity are maximal but decrease as a function of time, reflecting active unimer exchange between micelles. At $t = \infty$, the labeled polymers are entirely redistributed between micelles such that the contrast vanishes and the scattered intensity is at minimum.[25,26,31] Figure 2a shows a scattering curve measured at 20 °C of a 0.5 vol % PEP1-PEO20 solution containing 2.3 mg/mL SDS 48 h after mixing equal amounts of D and H labeled micellar reservoirs. In addition, a calculated average of the two individual curves of H and D micelles is shown, representing the initial scattering at t = 0. Figure 2a also shows the scattering data for a randomized mixture of the two components. This profile would appear if there was a complete mix in the system. As seen, the scattering curve after 48 h falls on top of the calculated average and does not approach the intensity of the randomized mixture. This is also not the case after measuring an extended period of time of 5 days. This becomes obvious from the constant detector count shown in Figure 2b. Apparently, polymer chain exchange does not take place, analogous to pure PEP1-PEO20 micelles without SDS.

In a previous work, it was shown that dimethylformamide (DMF) could activate the chain exchange in PEP1-PEO20 micelles, an effect that was attributed to the reduction of interfacial tension between the hydrophobic polymer block and the solvent.[25,26] Clearly, from the experimental data in the present work, the surfactant SDS does not give sufficient reduction in the activation energy to activate unimer exchange within 5 days. This is at odds with a previous finding by van Stam et al.[29] and Schantz et al.,[30] who both found that the rate of unimer exchange is accelerated by surfactants by the same extent as with cosolvents. Hecht et al.[32] studied the relaxation rate by light scattering in a system of Pluronic micelles and SDS and DTAB (dodecyltrimethylammonium bromide) and found that the fast relaxation constant ascribed to the unimer exchange increased with increasing surfactant concentration. However, given that the cores in Pluronic micelles contain a significant amount of water[47] due to the marginally hydrophobic poly(propylene oxide) (PPO) block, which is not surprising. It is probable that the molecular weight and surface tension of the PEP hydrophobic block in the present case are too large to be able to be effectively solubilized by the surfactant.

Our results suggest that PEP1-PEO20 polymer chains are not redistributed among the micelles; however, the small change in intensity observed in Figure 1 is due to the insertion of SDS surfactants. More insight can be obtained by a detailed analysis of the SAXS data by the mixed micelle structural model. The aggregation number of SDS after 5 days is concentration-dependent and is 150 for 2.33 mg/mL SDS and 125 for 1.67 mg/mL SDS. See additional data in Figure S.2 in the Supporting Information (SI). This indicates that the surfactants are incorporated into the PEP1-PEO20 micelles without activating the chain exchange. For the initial structure after 3 min, we additionally see from the inset in Figure 1b and the Supporting Information that the fit of the MM model is poor in the low Q region, especially for the low concentrations. We speculate that the intensity increase in the initial state is due to an inhomogeneous environment, where the micelles reorganize into a homogenous state in a time period of less than 1 h. The timescale here is surprising, as SDS exhibits molecular exchange dynamics in the order of microseconds.[22−24] In any case, the

https://dx.doi.org/10.1021/acs.langmuir.0c02123
Langmuir 2020, 36, 12887−12899

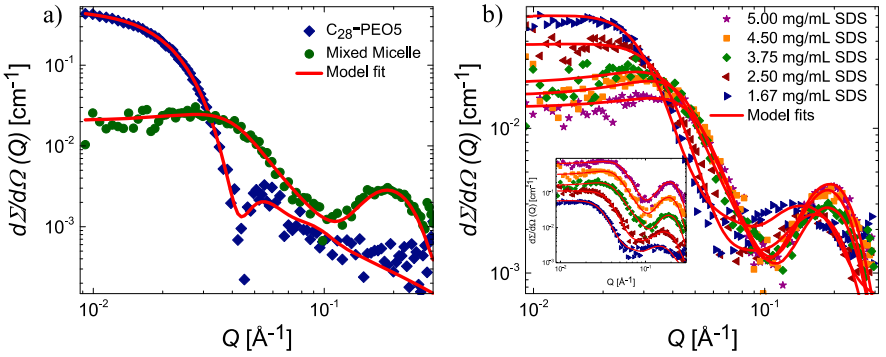

Figure 3. (a) SAXS scattering curves of 5.00 mg/mL C_{28}-PEO5 with core−shell model fit, and equilibrated mixture of 5.00 mg/mL C_{28}-PEO5 + 3.75 mg/mL SDS, fitted with the new MM model. (b) SAXS scattering curves of equilibrated 5.00 mg/mL C_{28}-PEO5 mixed with various concentrations of SDS. A clear trend toward smaller micelles with larger SDS concentration can be seen. The inset in (b) provides scaled scattering data to show the shift to higher Q values with higher concentrations of SDS.

Table 2. Structural Parameters of the Pure PEP1-PEO20 Micelle and the Mixture with SDS[a]

micelle	N_{agg} 3 min	N_{agg} 5 days	N^{P}_{agg}	R_m [Å] 3 min	R_m [Å] 5 days	R_c [Å] 3 min	R_c [Å] 5 days
PEP1-PEO20	78 ± 3	78 ± 3	78 ± 3	268 ± 6	268 ± 6	33 ± 1	33 ± 1
PEP1-PEO20 + 1.16 mg/mL SDS	258 ± 15	106 ± 14	78 ± 3	262 ± 6	277 ± 6	38 ± 1	35 ± 1
PEP1-PEO20 + 2.33 mg/mL SDS	253 ± 15	122 ± 14	78 ± 3	261 ± 6	280 ± 6	38 ± 1	35 ± 1

[a]The large uncertainties in the aggregation number are due to the small size of the SDS molecules in comparison to the micelles. However, the trend with larger micelle at the initial timepoint is clear.

results from scattering experiments on the PEP1-PEO20 system demonstrate that no major structural change takes place in the PEP1-PEO20 micelles with the addition of SDS. From the fit results, we see that the surfactants are simply inserted into the polymeric micelles. The micelles keep their structural integrity, where the aggregation number of the PEP1-PEO20 chains is constant to 78, and the chain exchange is not activated, as shown by SANS. The amount of surfactant inserted into the micelles varied from 0 at the lower concentrations, up to a fraction of 0.75 at 3 min after mixing and 0.40 after 5 days.

SAXS Characterization of *n*-Alkyl-PEO Micelles upon the Addition of SDS. In order to study the solubilization further, we proceeded to investigate *n*-alkyl-PEO, belonging to the group of hydrophobically end-capped polymers,[39] which are known to exhibit active molecular exchange kinetics in the order of minutes to hours at ambient temperatures.[27] As described previously, we have used C_{28}-PEO5, where the concentration was kept constant at 5.00 mg/mL, and the SDS concentrations were 1.67, 2.50, 3.75, 4.5, and 5.00 mg/mL. These concentrations were based on comparative molar volumes and molar ratios with the PEP1-PEO20 and SDS systems, where the 2.5 mg/mL concentration of SDS corresponds to a molar ratio of SDS/C_{28}-PEO5 of 9.3. An important note here is that the cmc of SDS is 8.0 mM,[48] i.e., 2.3 mg/mL at 20 °C, and the kinetics will be accordingly measured both above and below the cmc. Figure 3a shows the SAXS data of unmixed C_{28}-PEO5 as well as a mixture of C_{28}-PEO5 and SDS. Figure 3b shows the SAXS data for 5.0 mg/mL C_{28}-PEO5 at 69 h after mixing with various amounts of SDS to a polymer concentration of 5.0 mg/mL. As seen, the scattered intensity at low Q becomes progressively smaller with increasing amounts of SDS, indicating that the volume of the micelles is reduced. The obtained differences in this system are much larger than what was seen for PEP1-PEO20 mixed with SDS.

In order to extract detailed structural information from the scattering curves, the data were analyzed using the core−shell−corona model introduced in the theoretical section. As seen from the experimental results, the model can accurately describe the data, providing detailed structural information as summarized in Table 2. As suspected, the aggregation number of the polymer (N^{P}_{agg}) in the mixed micelles decreases with increasing SDS addition, whereas that of the SDS (f_{SDSm}) follows the opposite trend. This is in accordance with previous findings for copolymer and surfactant mixtures.[1,7−11,14−17]

Interestingly, the relation between the PEO corona thickness, D, and the aggregation number of the polymer, N^{P}_{agg}, follows the predicted scaling law for star-like micelles by Halperin and Alexander[39,49] $D \propto N^{P}_{agg}{}^{1/5}$ as shown in Figure 4. This suggests

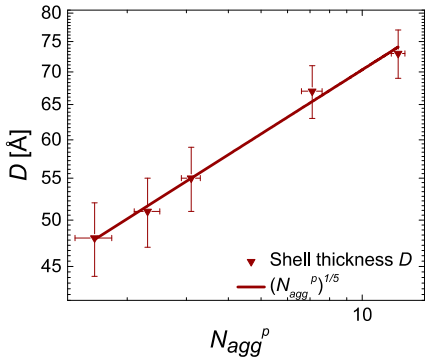

Figure 4. Halperin plot of shell thickness D versus aggregation number of the polymer $N_{agg}{}^{P}$ for each measured mixture of C_{28}-PEO5 and SDS at various concentrations.

that in the mixed micelles with SDS, the PEO chain interactions within the corona dominates following the behavior of star-like micelles. However, SDS molecules clearly are inserted into the interface and create more space between the grafted polymer chains, relieving the interactions.

Kinetics of Solubilization: *n*-Alkyl-PEO/SDS Mixtures. The C_{28}PEO5/SDS mixtures were measured continuously over

https://dx.doi.org/10.1021/acs.langmuir.0c02123
Langmuir 2020, 36, 12887−12899

69 h to observe the structural transition to smaller mixed micelles in situ. Selected scattering data for various mixtures obtained at different times are shown in Figure 5. See more results in Figure S.4 in the Supporting Information.

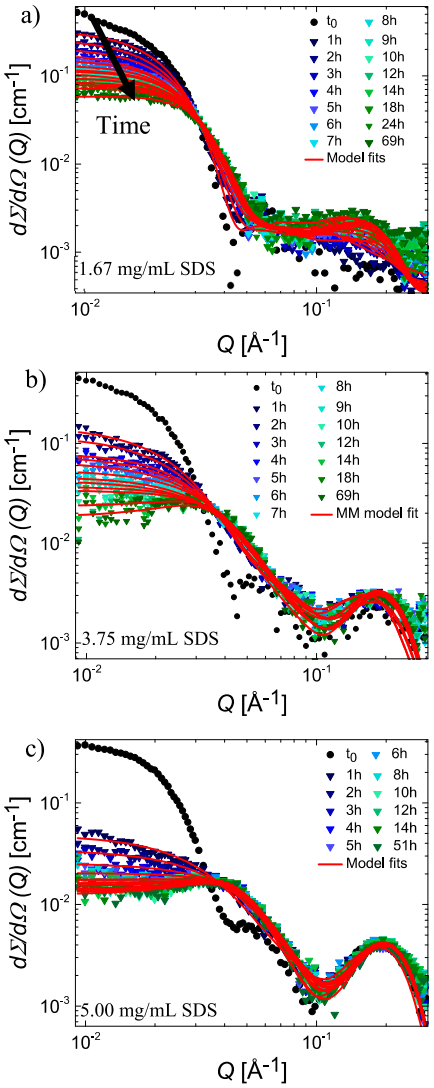

Figure 5. SAXS scattering curves over time for 5.00 mg/mL C_{28}-PEO5 mixed with (a) 1.67 mg/mL SDS, (b) 3.75 mg/mL SDS, and (c) 5.00 mg/mL SDS.

The intensity at low Q values is seen to decrease gradually over time. However, it is clear that we do not capture the very first part of the solubilization within the instrumental timescale. This gap increases with the SDS concentration, as the solubilization process becomes faster. In order to analyze the data more quantitatively, we first performed a model-independent Guinier analysis to obtain the intensity at low Q, $I(0)$, and the radius of gyration, R_g, which are proportional to the aggregation number and the overall size of the mixed micelles, respectively. The results can be found in the Supporting Information (Figure S.3). The resulting data show a decay in intensity that can be described by two exponentials indicating two main processes of rearrangement. However, as evident from the scattering curves for SDS-rich mixtures, the data gradually display a structure factor peak at longer times due to increasing micellar density and intermicellar repulsions, such that a model-independent Guinier fit is inappropriate. Thus, in order to quantify the solubilization process more accurately, we employed the mixed micelle scattering model where we varied the aggregation number of the polymer (N^{P}_{agg}) and the fraction of SDS in the mixed micelles (f_{SDSm}) over time. An attempt to include polydispersity in the aggregation number and composition, as realistically expected, failed as it led to increasing ambiguity in the fits due to the larger set of correlated variables. Nevertheless, the resulting fit quality shown in Figure 5 is satisfactory, and the time evolution of the resulting parameters are shown in Figure 6. Here, a kinetic model was fitted to the structural parameters in order to analyze the time evolution for N^{P}_{agg} and f_{SDSm}. As a starting point, a single exponential was employed; however, this could not capture the whole range, particularly the fast decay at the beginning of the process. Instead, a sum of two exponential functions was found to describe the data perfectly, indicating a "fast" process and a "slow" process:

$$N^{P}_{agg}(t) = N^{P}_{agg}(\infty) + (N^{P}_{agg}(0) - N^{P}_{agg}(\infty))\cdot \left(f_{fast}\exp\left(-\frac{1}{\tau_{fast}}t\right) + (1 - f_{fast})\exp\left(-\frac{1}{\tau_{slow}}t\right)^{\beta}\right) \quad (11)$$

where $N^{P}_{agg}(\infty)$ is the aggregation number of the polymer in the final state (shown in Table 3). $N^{P}_{agg}(0)$ is the aggregation number of the polymer in the initial state and was set to 95. This was found by fitting SAXS data of C_{28}-PEO5 with a core−shell model, consistent with what was found earlier.[35] f_{fast} is the

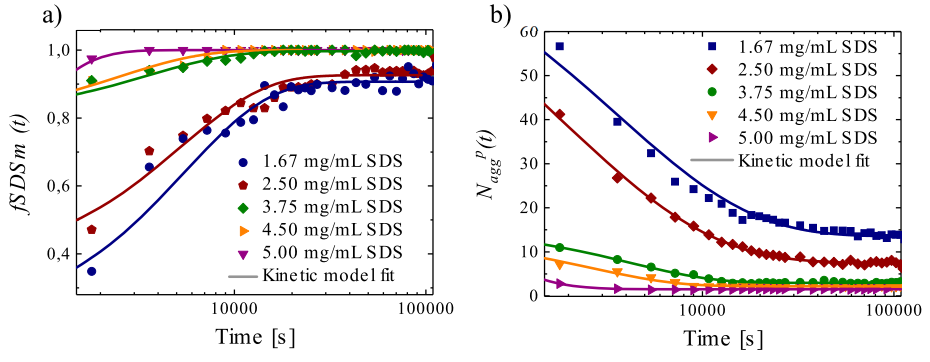

Figure 6. Evolution of the structural parameters on a logarithmic scale where C_{28}-PEO5 was held constant at 5.00 mg/mL and SDS varied: (a) fraction of SDS in the mixed micelles (f_{SDSm}) and (b) aggregation number of polymer ($N^{P}_{agg}(t)$) over time, fitted with the kinetic model.

https://dx.doi.org/10.1021/acs.langmuir.0c02123
Langmuir 2020, 36, 12887−12899

Table 3. Fit Results of Equilibrated Mixed Micelles of 5.00 mg/mL C_{28}-PEO5 and Various Concentrations of SDS

SDS [mg/mL]	N_{agg}	N^{p}_{agg}	R_m [Å]	R_c [Å]	D [Å]	f_{SDSm}
1.67	66 ± 3	12.8 ± 0.6	92 ± 4	19 ± 1	73 ± 4	0.96 ± 0.02
2.50	45 ± 3	7.1 ± 0.5	84 ± 4	17 ± 1	67 ± 4	0.96 ± 0.02
3.75	42 ± 3	3.1 ± 0.2	71 ± 4	16 ± 1	55 ± 4	1.00 ± 0.02
4.50	38 ± 3	2.3 ± 0.2	66 ± 4	15 ± 1	51 ± 4	1.00 ± 0.02
5.00	28 ± 3	1.6 ± 0.2	62 ± 4	14 ± 1	48 ± 4	1.00 ± 0.02

Table 4. Overview of Fitting Parameters in the Kinetic Model for N^{p}_{agg} and f_{SDSm}. The Concentration of C_{28}-PEO5 Was Kept Constant at 5.00 mg/mL[a]

	N^{p}_{agg}				f_{SDSm}			
SDS [mg/mL]	$N^{p}_{agg}(\infty)$ (fixed)	f_{fast}	τ^{m}_{slow} [s]/10^2	β	$f_{SDSm}(\infty)$ (fixed)	f_{fast}	τ^{m}_{slow} [s]/10^2	$\beta_{f_{SDSm}}$
1.67	12.8 ± 0.6	0.10 ± 0.01	49 ± 3	0.73	0.96 ± 0.02	0.21 ± 0.01	50 ± 3	0.80
2.50	7.1 ± 0.5	0.40 ± 0.02	45 ± 3	0.79	0.96 ± 0.02	0.39 ± 0.02	49 ± 3	0.83
3.75	3.1 ± 0.2	0.82 ± 0.04	35 ± 2	1	1.00 ± 0.02	0.80 ± 0.05	35 ± 2	1
4.50	2.3 ± 0.2	0.88 ± 0.04	26 ± 2	1	1.00 ± 0.02	0.84 ± 0.05	25 ± 2	1
5.00	1.6 ± 0.2	1.00 ± 0.05	2.8 ± 0.2[a]	0.70	1.00 ± 0.02	1.00 ± 0.05	5.3 ± 0.3[a]	1

[a]Merged process.

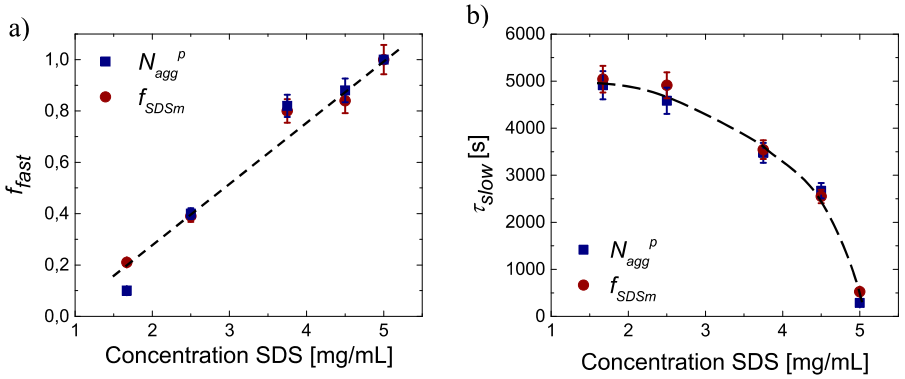

Figure 7. (a) Fraction of the fast process. (b) Obtained rate constant for the second process for a constant concentration of 5.00 mg/mL C_{28}-PEO5 mixed with various concentrations of SDS. A trend line is added to emphasize the trends with SDS concentration.

fraction of the fast process, τ_i (i = fast, slow) is the rate constant for the fast and slow process, and β is a measure of the distribution of the slow rate constant. The time evolution of f_{SDSm} can be similarly parameterized using the following equation:

$$f_{SDSm}(t) = f_{SDSm}(\infty)\left[\left(f_{fast}\cdot\exp\left(-\frac{t}{\tau_{fast}}\right)\right) + (1 - f_{fast})\cdot \exp\left(-\frac{t}{\tau_{slow}}\right)^{\beta_{f_{SDSm}}}\right] \quad (12)$$

where $f_{SDSm}(\infty)$ is analogous to $N^{p}_{agg}(\infty)$ in the final structure. The average relaxation time can then be calculated according to:

$$\tau^{m}_{slow} = \frac{\tau_{slow}}{\beta}\Gamma\left(\frac{1}{\beta}\right) \quad (13)$$

where Γ is the gamma function. τ_{fast} cannot be resolved with this time resolution and was thus set constant at an (arbitrary) value of 1 s for all concentrations except the highest where the "fast" and "slow" merged into one process. Constant values in the fitting procedure were $N^{p}_{agg}(0) = 95$ (from fitting with the core–shell model), and $f_{SDSm}(0) = 0$. τ_{fast} was held constant at 1 for both N^{p}_{agg} and f_{SDSm}. An overview of the result of the fitting is shown in Table 4. Figure 7 shows the plots for how the fraction of the fast process and the rate constant for the slow process depend on SDS concentration.

To obtain estimates of the uncertainty in the results, the experiment was repeated three times for the mixture of 8.00 mg/mL C_{28}-PEO5 and 4.00 mg/mL SDS. Based on this, a standard deviation was obtained which was used as an estimate of uncertainty.

Unfortunately, the rate constant for the fast process could not be resolved with this experimental setup, and τ_{fast} has been set constant to 1 in the fitting procedure of the kinetic data. f_{fast} was found to be 1 for 5.00 mg/mL SDS for both f_{SDSm} and N^{p}_{agg}. Both parameters could be fitted with a single exponential at this concentration, and the given rate constant is that of the single exponential. This could either be because we are not able to resolve the two different processes or because another process is occurring at this high SDS concentration. The data also clearly show that the fraction of the fast process increases nearly linearly with concentration before the two processes merge into one at the highest SDS content. Furthermore, the rate of the slow process is greatly accelerated, indicating that the barrier for molecular rearrangement processes is greatly reduced upon adding surfactants.

These results suggest that the "fast" process corresponds to a fast "solubilization" step where surfactant molecules are inserted

https://dx.doi.org/10.1021/acs.langmuir.0c02123
Langmuir 2020, 36, 12887−12899

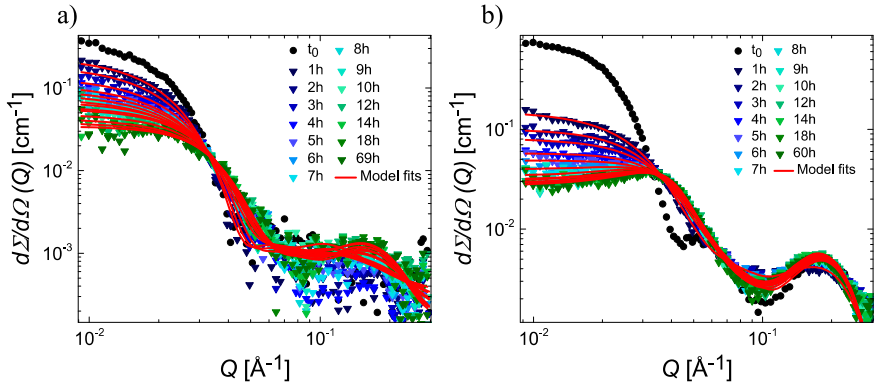

Figure 8. SAXS scattering curves of (a) 3.75 mg/mL C_{28}-PEO5 and 1.88 mg/mL SDS and (b) 10.0 mg/mL C_{28}-PEO5 and 5.00 mg/mL SDS at 20 °C.

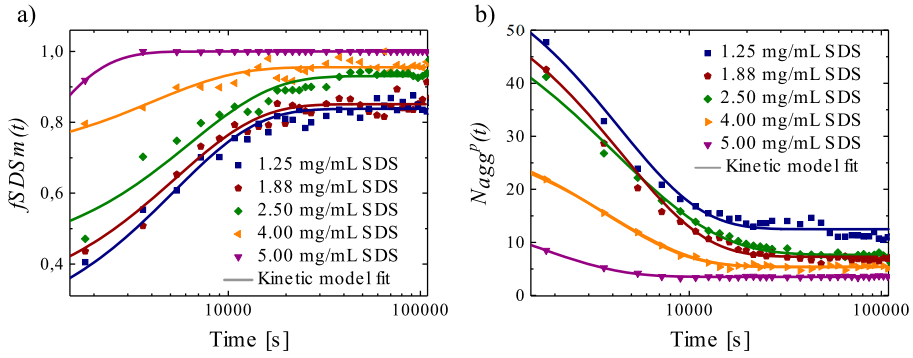

Figure 9. Evolution of the structural parameters on a logarithmic time scale where the molar ratio SDS/C_{28}-PEO5 was held constant at 9.3. The concentration of C_{28}-PEO5 is the double of the given concentrations of SDS. (a) Fraction of SDS in the mixed micelles (f_{SDSm}) and (b) aggregation number of polymer ($N^{p}_{agg}(t)$) over time, fitted with the kinetic model.

Table 5. Overview of Fitting Parameters in the Kinetic Model for N^{p}_{agg} and f_{SDSm}. The Total Concentration Consists of both SDS and C_{28}-PEO5, Where the Concentration of C_{28}-PEO5 Is Twice the Concentration of SDS

	N^{p}_{agg}				f_{SDSm}			
total conc. [mg/mL]	$N^{p}_{agg}(\infty)$ (fixed)	f_{fast}	τ^{m}_{slow} [s]/10^2	β	$f_{SDSm}(\infty)$ (fixed)	f_{fast}	τ^{m}_{slow} [s]/10^2	$\beta_{f_{SDSm}}$
3.75	11.4 ± 0.6	0.37 ± 0.02	43 ± 3	0.96	0.88 ± 0.02	0.34 ± 0.02	50 ± 3	0.92
5.63	6.9 ± 0.5	0.40 ± 0.02	44 ± 3	0.96	0.89 ± 0.02	0.33 ± 0.02	52 ± 3	0.95
7.50	7.1 ± 0.5	0.41 ± 0.02	46 ± 3	0.79	0.96 ± 0.02	0.39 ± 0.02	49 ± 3	0.83
12.0	5.3 ± 0.3	0.72 ± 0.04	40 ± 3	1	0.97 ± 0.02	0.73 ± 0.04	40 ± 3	1
15.0	3.6 ± 0.2	0.84 ± 0.05	16 ± 1	1	1.00 ± 0.02	0.80 ± 0.05	15 ± 1	1

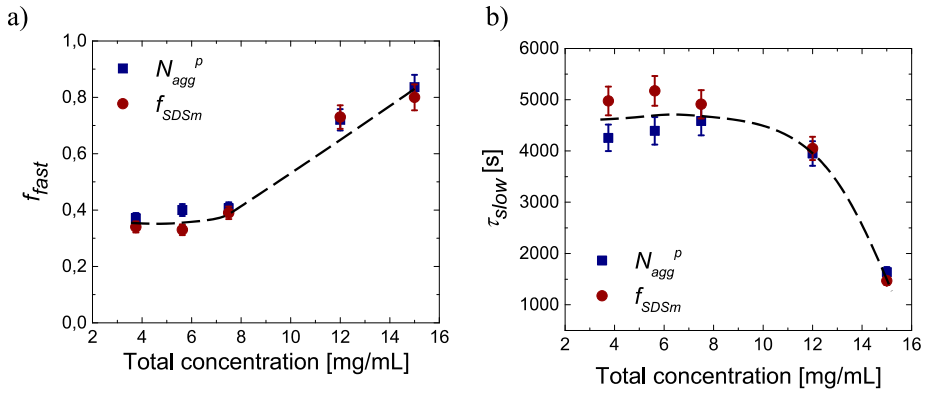

Figure 10. (a) Fraction of the fast process (b) Obtained rate constant for the second process for a constant ratio of SDS to C_{28}-PEO5 of 9.3, where the total concentration is varied.

and fragment parts of the polymer micelle, i.e., in a fission/fragmentation step. The much slower (10−20-fold) second process may be due to structural rearrangements where the polymer chains are exchanged in a gradual equilibration process.

https://dx.doi.org/10.1021/acs.langmuir.0c02123
Langmuir 2020, 36, 12887−12899

This bears similarity to morphological transitions in PEP-PEO micelles[38] and other block copolymers systems. In the present system, the micellar corona becomes diluted, i.e., as surfactant molecules are inserted and the polymer grafting density decreases over time. This might lead to an increased occurrence of fusion events. Thus, in order to further investigate the process, we performed a new set of experiments where the total concentration was varied. Selected scattering curves (see more in Figure S.5 in the Supporting Information) are shown in Figure 8 for SDS/C_{28}-PEO5 mixtures fixed at a molar ratio of 9.3. The same analysis as done before was applied, leading to a satisfactory quality of the fit.

The obtained rate constants for the slow process and the fraction of the fast process, according to the model described above, are shown in Figure 9. Again, the rate constant for the fast process was too fast to be resolved, and constant values in the fitting procedure were $N^{p}_{agg}(0) = 95$ (from fitting with core−shell model), $f_{SDSm}(0) = 0$, and $\tau_{fast} = 1$ for both N^{p}_{agg} and f_{SDSm}. An overview of the resulting fit parameters is given in Tables 4 and 5.

As can be seen in Figure 10, the data show a near constant f_{fast} at low concentrations for both $f_{SDSm}(t)$ and $N^{p}_{agg}(t)$. Moreover, the time constant for the slow process is also nearly constant in this range. It is interesting to note that there is a clear difference at low concentrations with respect to the case where the polymer concentration was held fixed and the surfactant content varied (Figure 7). At higher concentrations, the time constants merge and quickly drop (Figure 10b). Interestingly, the breakpoint happens at about 7 to 8 mg/mL in total concentration, which coincides with the nominal cmc of the pure surfactant solution. This may indicate that the accelerated kinetics is related to increased cooperativity in the fragmentation process upon crossing the cmc. Furthermore, the critical aggregation concentration (cac) of SDS may be different to the cmc, as there are also polymers present in the system. These results show that the solubilization process is in fact a combination of two processes, which is at odds with the findings by Cerritelli et al.,[33] who found first-order kinetics with only monomers of the surfactant interacting with the polymer micelles as the rate leveled off near the cmc. In our study, we see a significant acceleration for both concentration studies above the cmc, indicating a fusion/fission mechanism between the surfactant and polymer micelles.

Mechanism for Solubilization and Hybrid Micelle Formation. The results presented in this study show that the rate of solubilization is highly dependent on the length of the core-forming block, where SDS does not solubilize PEP1-PEO20 on a practical timescale, whereas it does solubilize C_{28}-PEO5 in the order of 5−10 h. The initial step is probably an insertion of SDS into the core−corona interface, as deduced from the results obtained on the PEP1-PEO20 system. The driving force for insertion is most likely the entropy of mixing in the system, as well as a decrease of the interfacial tension between the hydrophobic block and the solvent. If the hydrophobic block is too large, SDS is not capable of solubilizing the micelle, and the system reorganizes into mixed micelles. The impact of the size of the hydrophobic core was also seen in other copolymer/surfactant systems, such as for Pluronics and bile salts. Here it was seen that micelles with larger hydrophobic cores are not fully disintegrated, whereas micelles with smaller hydrophobic cores are fully solubilized.[15−17] A complicated hydrophobic interaction between surfactants and micelles was also reported by Wang et al.[18] Using a double chain surfactant, they found a stronger but more complicated interaction with the micelles than with single chain surfactants. The used surfactant does not completely break down Pluronic micelles with higher PO/EO ratio (P123), but it completely breaks down F123 with a smaller PO/EO ratio. For micelles with a shorter hydrophobic block, the next step is a fast process, possibly involving a fragmentation/fission step. The contribution from the fast process increases linearly with higher amounts of SDS. It must be pointed out that the fast rate constant could not be resolved here, and it is, therefore, not possible to determine its concentration dependence. Dormidontova et al.[50] showed that the free energy of fission is negative when $N_{agg}(\text{initial}) > 2N_{agg}(\text{eq})$ as the initial micelle can split into symmetrical micelles in order to get to the equilibrium structure. $N^{p}_{agg}(0) = 95$ at the initial state of C_{28}-PEO5, and $N^{p}_{agg}(\infty)$ was observed to become more than half of that the initial state for the final state when the amount of SDS was 2.5 mg/mL and higher. Based on this reasoning, fission/fragmentation could be a possible mechanism for the solubilization for 2.5 mg/mL SDS and higher concentrations. It is interesting to note that the fraction of the fast process is small at low surfactant concentrations, where fusion/fission events are less likely to occur. This indicates a surfactant-mediated fission/fragmentation process. Pool et al.[51] performed a simulation of surfactant formation around the cmc and reported that growing micelles could become unstable and split into two similar-sized micelles. They report that this phenomenon gives a significant contribution to the formation mechanism of surfactant micelles in addition to the well-known nucleation and growth mechanism.[51] A possible mechanism for the fast solubilization step found in the present study could be that mixed micelles grow because SDS was inserted into the core very rapidly, after the micelles become unstable and fragment into smaller mixed micelles. Pizzirusso et al.[52] have studied the solubilization process of lipid bilayers by a coarse-grained model simulation on liposomes with Triton X-100 (neutral) surfactant. Even though the present study is performed on a quite different system, some insight might be transferred to ours. The breakup of the liposomes can occur by either a fast or a slow process, explained by a three-step-model.[52] The fast process occurs for systems with the rapid flip-flop of the lipid chains. As flip-flop does not occur in micellar systems, it is more reasonable to examine the driving force for the slow process of solubilization for lipids. When surfactants are inserted into the bilayer, they demand space, and an unfavorable curvature emerges, which causes the bilayers to break down. A similar process could possibly occur in polymer systems as well. We showed in the work performed on PEP1-PEO20 and SDS that the aggregation number of the surfactant is higher in the initial state than the final state, which means that the majority of surfactant molecules are inserted into the core very rapidly. Large electrostatic repulsion between the surfactant heads could then occur due to crowding in the core−shell interface of the micelles. The repulsion between the surfactant heads can then drive the micelle to initially swell and then break up and fragment into smaller micelles, as long as the hydrophobic chain is not too large. Another destabilizing mechanism is found in other polymer systems; among them, Rayleigh instability is found in PEP1-PEO20,[38] where fluctuations in the surface cause the structure to break down. A combination of Rayleigh instability together with the effect seen in liposomes could thus be a possibility because of the decreased surface tension by SDS in the interface, which would cause more fluctuations in the core−shell interface. However, the timescale of the fast process is surprising, as Rayleigh instability occurs in the order of

https://dx.doi.org/10.1021/acs.langmuir.0c02123
Langmuir 2020, 36, 12887−12899

milliseconds to seconds. This would indicate a high activation barrier in our system. A difference to the Rayleigh instability found in PEP1-PEO20[38] is that the latter was a cylindrical system where fluctuations can more easily cause an unfavorable curvature. The present system is spherical, which could be the reason for the slow timescale of the process. However, as the initial stages of solubilization was not captured by this instrumental setup, we do not have sufficient information to form conclusions regarding this question.

Here, the slow process is reported to be independent of concentration up to a certain concentration threshold, which seems to correlate with the cmc of pure SDS. This result indicates that chain exchange is the main mechanism at low concentrations. This result is in accordance with previous research on hybridization of different block copolymer micelles by Tian et al.[19] and previous work on PEP-PEO systems.[38] At higher surfactant concentrations, we see a concentration dependence, indicating that fusion/fission occurs—in accordance with the work by Schantz et al.[30]—as the main mechanism to form monodisperse and homogeneous micelles. One possible explanation for the small fraction of the slow process (large fraction for the fast process) for high SDS concentrations is that the polymer micelles break down into smaller and more uniform micelles in the first step, reducing the need for a reorganization step.

Overall, based on the results from the present study, we postulate that the steps of solubilization of polymeric micelles can be schematically illustrated as in Figure 11, where the two concentration regimes indicated are based on the increasing fraction of the fast process.

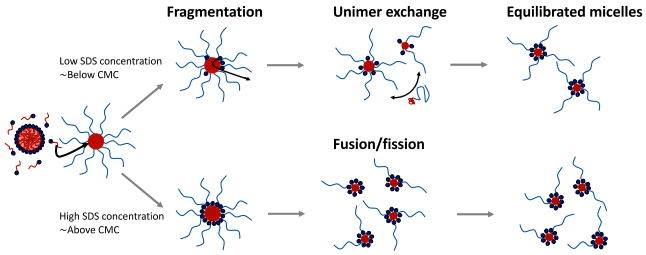

Figure 11. Schematic illustration of the break down of "living" micelles upon SDS addition.

CONCLUSIONS

In the present work, we have used a coexistence model for mixed micelles, surfactant micelles, and free surfactant chains to analyze the formation of mixed micelles over time after the addition of a surfactant to the solutions of polymer micelles. We found that for the polymer micelles, i.e., the PEP1-PEO20 system investigated in this work, solubilization with SDS was not found to occur for the SDS concentrations and timescale explored (5 days). This is likely due to the high interfacial tension and length of the hydrophobic block. For hybrid micelles, i.e., C_{28}-PEO5, mixed micelles with SDS were formed over the timescale of 5−10 h depending on the SDS concentration. The break down process was analyzed with a kinetic model containing two exponential functions and hence found to be a combination of two processes. The first process was found to be a fast solubilization process, which is highly dependent on concentration. Above the cmc, this step is the dominating process and is likely to be an insertion/fusion−fission step. The second process is a reorganization step, which at low concentrations of SDS is mostly mediated by unimer exchange, while at higher concentrations, it is a fusion/fission mechanism. Notwithstanding these results, more work would be needed to unravel the specific mechanism of the initial stages of the solubilization process. This may be achieved using TR-SAXS, which requires synchrotron radiation and a stopped-flow apparatus for rapid mixing.

ASSOCIATED CONTENT

Supporting Information

The Supporting Information is available free of charge at https://pubs.acs.org/doi/10.1021/acs.langmuir.0c02123.

Additional sample information; SAXS data; and fit analysis (PDF)

AUTHOR INFORMATION

Corresponding Author

Reidar Lund − *Department of Chemistry, University of Oslo, Oslo 0315, Norway*; orcid.org/0000-0001-8017-6396; Email: reidar.lund@kjemi.uio.no

Authors

Synne Myhre − *Department of Chemistry, University of Oslo, Oslo 0315, Norway*

Matthias Amann − *Department of Chemistry, University of Oslo, Oslo 0315, Norway*

Lutz Willner − *Jülich Centre for Neutron Science (JCNS-1) and Institute of Biological Information Processing (IBI-8) Forschungszentrum Jülich GmbH, Jülich 52425, Germany*

Kenneth D. Knudsen − *IFE, Institute for Energy Technology, Kjeller 2007, Norway*

Complete contact information is available at: https://pubs.acs.org/10.1021/acs.langmuir.0c02123

Notes

The authors declare no competing financial interest.

ACKNOWLEDGMENTS

The authors acknowledge the European Synchrotron Radiation Facility ESRF for the provision of synchrotron radiation beamtime at the BM29 instrument. The authors also acknowledge the use of the Norwegian National Infrastructure for X-ray diffraction and scattering (RECX) and the Institute for Energy Technology (IFE) for the use of the SANS instrument. The authors dedicate this work to the memory of Matthias Amann, who tragically passed away during the preparation of this manuscript.

REFERENCES

(1) Jansson, J.; Schillén, K.; Olofsson, G.; Cardoso da Silva, R.; Loh, W. The Interaction between PEO-PPO-PEO Triblock Copolymers and Ionic Surfactants in Aqueous Solution Studied Using Light Scattering and Calorimetry. *J. Phys. Chem. B* **2004**, *108*, 82−92.

(2) Kataoka, K.; Harada, A.; Nagasaki, Y. Block copolymer micelles for drug delivery: Design, characterization and biological significance. *Adv. Drug Delivery Rev.* **2012**, *64*, 37−48.

(3) Nagarajan, R., Polymer-Surfactant Interactions. *New Horizons: Detergents for the New Millennium Conference Invited Papers* 2001.

(4) Lochhead, R. Y., The Role of Polymers in Cosmetics: Recent Trends. In *Cosmetic Nanotechnology*, American Chemical Society: 2007; *961*, 3−56.

(5) Narayanan, T.; Wacklin, H.; Konovalov, O.; Lund, R. Recent applications of synchrotron radiation and neutrons in the study of soft matter. *Crystallogr. Rev.* **2017**, *23*, 160−226.
(6) Sastry, N. V.; Hoffmann, H. Interaction of amphiphilic block copolymer micelles with surfactants. *Colloids Surf. A: Physicochem. Eng. Aspects* **2004**, *250*, 247−261.
(7) Hecht, E.; Hoffmann, H. Interaction of ABA block copolymers with ionic surfactants in aqueous solution. *Langmuir* **1994**, *10*, 86−91.
(8) Hecht, E.; Mortensen, K.; Gradzielski, M.; Hoffmann, H. Interaction of ABA Block Copolymers with Ionic Surfactants: Influence on Micellization and Gelation. *J. Phys. Chem.* **1995**, *99*, 4866−4874.
(9) Jansson, J.; Schillén, K.; Nilsson, M.; Söderman, O.; Fritz, G.; Bergmann, A.; Glatter, O. Small-Angle X-ray Scattering, Light Scattering, and NMR Study of PEO−PPO−PEO Triblock Copolymer/Cationic Surfactant Complexes in Aqueous Solution. *J. Phys. Chem. B* **2005**, *109*, 7073−7083.
(10) Cardoso da Silva, R.; Olofsson, G.; Schillén, K.; Loh, W. Influence of Ionic Surfactants on the Aggregation of Poly(Ethylene Oxide)−Poly(Propylene Oxide)−Poly(Ethylene Oxide) Block Copolymers Studied by Differential Scanning and Isothermal Titration Calorimetry. *J. Phys. Chem. B* **2002**, *106*, 1239−1246.
(11) Li, Y.; Ghoreishi, S. M.; Warr, J.; Bloor, D. M.; Holzwarth, J. F.; Wyn-Jones, E. Interactions between a Nonionic Copolymer Containing Different Amounts of Covalently Bonded Vinyl Acrylic Acid and Surfactants: EMF and Microcalorimetry Studies. *Langmuir* **1999**, *15*, 6326−6332.
(12) Almgren, M.; Van Stam, J.; Lindblad, C.; Li, P.; Stilbs, P.; Bahadur, P. Aggregation of poly(ethylene oxide)-poly(propylene oxide)-poly(ethylene oxide) triblock copolymers in the presence of sodium dodecyl sulfate in aqueous solution. *J. Phys. Chem.* **1991**, *95*, 5677−5684.
(13) Bronstein, L. M.; Chernyshov, D. M.; Timofeeva, G. I.; Dubrovina, L. V.; Valetsky, P. M.; Khokhlov, A. R. The Hybrids of Polystyrene-block-Poly(ethylene Oxide) Micelles and Sodium Dodecyl Sulfate in Aqueous Solutions: Interaction with Rh Ions and Rh Nanoparticle Formation. *J. Colloid Interface Sci.* **2000**, *230*, 140−149.
(14) Cantú, L.; Corti, M.; Salina, P. Direct measurement of the formation time of mixed micelles. *J. Phys. Chem.* **1991**, *95*, 5981−5983.
(15) Bayati, S.; Galantini, L.; Knudsen, K. D.; Schillén, K. Effects of Bile Salt Sodium Glycodeoxycholate on the Self-Assembly of PEO-PPO-PEO Triblock Copolymer P123 in Aqueous Solution. *Langmuir* **2015**, *31*, 13519−13527.
(16) Bayati, S.; Anderberg Haglund, C.; Pavel, N. V.; Galantini, L.; Schillén, K. Interaction between bile salt sodium glycodeoxycholate and PEO−PPO−PEO triblock copolymers in aqueous solution. *RSC Adv.* **2016**, *6*, 69313−69325.
(17) Bayati, S.; Galantini, L.; Knudsen, K. D.; Schillén, K. Complexes of PEO-PPO-PEO triblock copolymer P123 and bile salt sodium glycodeoxycholate in aqueous solution: A small angle X-ray and neutron scattering investigation. *Colloids Surf., A* **2016**, *504*, 426−436.
(18) Wang, R.; Tang, Y.; Wang, Y. Effects of Cationic Ammonium Gemini Surfactant on Micellization of PEO−PPO−PEO Triblock Copolymers in Aqueous Solution. *Langmuir* **2014**, *30*, 1957−1968.
(19) Tian, M.; Qin, A.; Ramireddy, C.; Webber, S. E.; Munk, P.; Tuzar, Z.; Prochazka, K. Hybridization of block copolymer micelles. *Langmuir* **1993**, *9*, 1741−1748.
(20) Bronstein, L. M.; Chernyshov, D. M.; Timofeeva, G. I.; Dubrovina, L. V.; Valetsky, P. M.; Khokhlov, A. R. Polystyrene-block-Poly(ethylene oxide) Micelles in Aqueous Solution. *Langmuir* **1999**, *15*, 6195−6200.
(21) Rehman, N.; Khan, A.; Bibi, I.; Bica, C. I. D.; Siddiq, M. Intermolecular Interactions of Polymer/Surfactants Mixture in Aqueous Solution Investigated by Various Techniques. *J. Dispers. Sci. Technol.* **2013**, *34*, 1202−1210.
(22) Schmölzer, S.; Gräbner, D.; Gradzielski, M.; Narayanan, T. Millisecond-Range Time-Resolved Small-Angle X-Ray Scattering Studies of Micellar Transformations. *Phys. Rev. Lett.* **2002**, *88*, 258301.
(23) Lang, J.; Tondre, C.; Zana, R.; Bauer, R.; Hoffmann, H.; Ulbricht, W. Chemical relaxation studies of micellar equilibriums. *J. Phys. Chem.* **1975**, *79*, 276−283.
(24) Aniansson, E. A. G.; Wall, S. N.; Almgren, M.; Hoffmann, H.; Kielmann, I.; Ulbricht, W.; Zana, R.; Lang, J.; Tondre, C. Theory of the kinetics of micellar equilibria and quantitative interpretation of chemical relaxation studies of micellar solutions of ionic surfactants. *J. Phys. Chem.* **1976**, *80*, 905−922.
(25) Lund, R.; Willner, L.; Stellbrink, J.; Lindner, P.; Richter, D. Logarithmic Chain-Exchange Kinetics of Diblock Copolymer Micelles. *Phys. Rev. Lett.* **2006**, *96*, No. 068302.
(26) Lund, R.; Willner, L.; Richter, D.; Dormidontova, E. E. Equilibrium Chain Exchange Kinetics of Diblock Copolymer Micelles: Tuning and Logarithmic Relaxation. *Macromolecules* **2006**, *39*, 4566−4575.
(27) Zinn, T.; Willner, L.; Lund, R.; Pipich, V.; Richter, D. Equilibrium exchange kinetics in n-alkyl−PEO polymeric micelles: single exponential relaxation and chain length dependence. *Soft Matter* **2012**, *8*, 623−626.
(28) Halperin, A.; Alexander, S. Polymeric micelles: their relaxation kinetics. *Macromolecules* **1989**, *22*, 2403−2412.
(29) van Stam, J.; Creutz, S.; De Schryver, F. C.; Jéröme, R. Tuning of the Exchange Dynamics of Unimers between Block Copolymer Micelles with Temperature, Cosolvents, and Cosurfactants. *Macromolecules* **2000**, *33*, 6388−6395.
(30) Schantz, A. B.; Saboe, P. O.; Sines, I. T.; Lee, H.-Y.; Bishop, K. J. M.; Maranas, J. K.; Butler, P. D.; Kumar, M. PEE−PEO Block Copolymer Exchange Rate between Mixed Micelles Is Detergent and Temperature Activated. *Macromolecules* **2017**, *50*, 2484−2494.
(31) Abe, A.; Lee, K. S.; Leibler, L.; Kobayashi, S.; Cai, C., *Controlled polymerization and polymeric structures : flow microreactor polymerization, micelles kinetics, polypeptide ordering, light emitting nanostructures*. Springer: Cham; New York, 2013; 248.
(32) Hecht, E.; Hoffmann, H. Kinetic and calorimetric investigations on micelle formation of block copolymers of the poloxamer type. *Colloids Surf. A: Physicochem. Eng. Aspects* **1995**, *96*, 181−197.
(33) Cerritelli, S.; Velluto, D.; Hubbell, J. A.; Fontana, A. Breakdown kinetics of aggregates from poly(ethylene glycol-bl-propylene sulfide) di- and triblock copolymers induced by a non-ionic surfactant. *J. Polym. Sci. Part A Polym. Chem.* **2008**, *46*, 2477−2487.
(34) Boldon, L.; Laliberte, F.; Liu, L. Review of the fundamental theories behind small angle X-ray scattering, molecular dynamics simulations, and relevant integrated application. *Nano Rev.* **2015**, *6*, 25661−25661.
(35) Narayanan, T.; Sztucki, M.; Van Vaerenbergh, P.; Léonardon, J.; Gorini, J.; Claustre, L.; Sever, F.; Morse, J.; Boesecke, P. A multipurpose instrument for time-resolved ultra-small-angle and coherent X-ray scattering. *J. Appl. Crystallogr.* **2018**, *51*, 1511−1524.
(36) Lund, R.; Willner, L.; Stellbrink, J.; Radulescu, A.; Richter, D. Role of Interfacial Tension for the Structure of PEP−PEO Polymeric Micelles. A Combined SANS and Pendant Drop Tensiometry Investigation. *Macromolecules* **2004**, *37*, 9984−9993.
(37) Lund, R.; Willner, L.; Monkenbusch, M.; Panine, P.; Narayanan, T.; Colmenero, J.; Richter, D. Structural Observation and Kinetic Pathway in the Formation of Polymeric Micelles. *Phys. Rev. Lett.* **2009**, *102*, 188301.
(38) Lund, R.; Willner, L.; Richter, D.; Lindner, P.; Narayanan, T. Kinetic Pathway of the Cylinder-to-Sphere Transition in Block Copolymer Micelles Observed in Situ by Time-Resolved Neutron and Synchrotron Scattering. *ACS Macro Lett.* **2013**, *2*, 1082−1087.
(39) Zinn, T.; Willner, L.; Lund, R.; Pipich, V.; Appavou, M.-S.; Richter, D. Surfactant or block copolymer micelles? Structural properties of a series of well-defined n-alkyl−PEO micelles in water studied by SANS. *Soft Matter* **2014**, *10*, 5212−5220.
(40) Zinn, T.; Willner, L.; Lund, R. Nanoscopic Confinement through Self-Assembly: Crystallization within Micellar Cores Exhibits Simple Gibbs-Thomson Behavior. *Phys. Rev. Lett.* **2014**, *113*, 238305.
(41) Zinn, T.; Willner, L.; Pipich, V.; Richter, D.; Lund, R. Effect of Core Crystallization and Conformational Entropy on the Molecular

Exchange Kinetics of Polymeric Micelles. *ACS Macro Lett.* **2015**, *4*, 651−655.
(42) Zinn, T.; Willner, L.; Pipich, V.; Richter, D.; Lund, R. Molecular Exchange Kinetics of Micelles: Corona Chain Length Dependence. *ACS Macro Lett.* **2016**, *5*, 884−888.
(43) König, N.; Willner, L.; Pipich, V.; Zinn, T.; Lund, R. Cooperativity during Melting and Molecular Exchange in Micelles with Crystalline Cores. *Phys. Rev. Lett.* **2019**, *122*, No. 078001.
(44) Pernot, P.; Round, A.; Barrett, R.; De Maria Antolinos, A.; Gobbo, A.; Gordon, E.; Huet, J.; Kieffer, J.; Lentini, M.; Mattenet, M. Upgraded ESRF BM29 beamline for SAXS on macromolecules in solution. *J. Synchrotron Rad.* **2013**, *20*, 660−664.
(45) Round, A.; Felisaz, F.; Fodinger, L.; Gobbo, A.; Huet, J.; Villard, C.; Blanchet, C. E.; Pernot, P.; McSweeney, S.; Roessle, M.; Svergun, D. I.; Cipriani, F. BioSAXS Sample Changer: a robotic sample changer for rapid and reliable high-throughput X-ray solution scattering experiments. *Acta Crystallogr. Sect. D Biol. Crystallogr.* **2015**, *71*, 67−75.
(46) Willner, L.; Poppe, A.; Allgaier, J.; Monkenbusch, M.; Richter, D. Time-resolved SANS for the determination of unimer exchange kinetics in block copolymer micelles. *Europhys. Lett. (EPL)* **2001**, *55*, 667−673.
(47) Pedersen, J. S.; Gerstenberg, M. C. The structure of P85 Pluronic block copolymer micelles determined by small-angle neutron scattering. *Colloids Surf. A Physicochem. Eng. Aspects* **2003**, *213*, 175−187.
(48) Inayathullah, N. M.; Jasmine, G. J.; Jayakumar, R. Effect of Osmolyte on the Micellization of SDS at Different Temperatures. *Langmuir* **2003**, *19*, 9545−9547.
(49) Halperin, A. Polymeric micelles: a star model. *Macromolecules* **1987**, *20*, 2943−2946.
(50) Dormidontova, E. E. Micellization Kinetics in Block Copolymer Solutions: Scaling Model. *Macromolecules* **1999**, *32*, 7630−7644.
(51) Pool, R.; Bolhuis, P. G. Prediction of an Autocatalytic Replication Mechanism for Micelle Formation. *Phys. Rev. Lett.* **2006**, *97*, No. 018302.
(52) Pizzirusso, A.; De Nicola, A.; Sevink, G. J. A.; Correa, A.; Cascella, M.; Kawakatsu, T.; Rocco, M.; Zhao, Y.; Celino, M.; Milano, G. Biomembrane solubilization mechanism by Triton X-100: a computational study of the three stage model. *Phys. Chem. Chem. Phys.* **2017**, *19*, 29780−29794.

https://dx.doi.org/10.1021/acs.langmuir.0c02123
Langmuir 2020, 36, 12887−12899